Chemical order and structure of the mechanically milled Fe_2Hf Laves phase

1998 J. Phys.: Condens. Matter 10 3457

(http://iopscience.iop.org/0953-8984/10/15/021)

J. Phys.: Condens. Matter **10** (1998) 3457–3466. Printed in the UK PII: S0953-8984(98)87597-8

Chemical order and structure of the mechanically milled Fe_2Hf Laves phase

S K Xia†, H Saitovitch†, P R J Silva†, J A Gomez†, F C Rizzo Assunção‡ and E Baggio-Saitovitch†

† Centro Brasileiro de Pesquisas Fisicas, Rua Dr Xavier Sigaud 150, 22290-160 Rio de Janeiro, RJ, Brazil

‡ DCMM, PUC-RIO, Rua Marquês de São Vicente 225, 22453-900 Rio de Janeiro, RJ, Brazil

Received 15 September 1997, in final form 22 January 1998

Abstract. The effects of mechanical milling on the chemical order and structure of the Fe_2Hf C14 Laves phase have been studied by x-ray diffraction and Mössbauer spectroscopy. The results show that ball milling leads to a segregation of two phases. One, with a lower degree of chemical disorder, maintains the structure of the original intermetallic phase and the other, with a higher degree of chemical disorder, exhibits a disordered structure. At 4.2 K, the two phases exhibit similar hyperfine magnetic fields which are smaller than that of the original intermetallic phase, but much larger than that of the amorphous alloy with the same composition, prepared by sputtering deposition. Differing from the crystalline phase, the structurally disordered phase shows a Curie temperature lower than room temperature.

1. Introduction

Mechanical milling (MM) is a technique for producing metastable phases. It has been shown that, upon MM, an intermetallic phase can transform to a chemically disordered or an amorphous phase [1–4] at temperatures near room temperature (RT). Some of these metastable phases prepared by MM have displayed interesting magnetic phenomena [5].

To have a better understanding of the physical properties of the powders prepared by MM, it is essential to study the MM induced atomic configurations including atomic coordination and local structures. In this work, we studied the atomic disordering, the structural variation and some magnetic properties of the mechanically milled Fe_2Hf C14-type Laves phase. The Fe_2Hf intermetallic phase is suited to the study because amorphous alloys can be obtained in this composition range by the gas condensation method [6]. Besides, the structures and the magnetic properties, especially the Mössbauer hyperfine parameters of the crystalline and amorphous Fe_2Hf alloys, have been well studied [6–8]. Our experimental results were obtained by x-ray diffraction (XRD) and Mössbauer spectroscopy (MS). Compared to XRD, which is related to the structural long-range-order, MS has the advantage of measuring the hyperfine parameters, which result from the local atomic configurations.

2. Experimental details

The ingot of Fe_2Hf intermetallic phase was prepared in an arc-melt furnace followed by a 100 h homogeneity annealing at 900 °C. The powders were prepared by SPEX-8000 mixer

0953-8984/98/153457+10$19.50

using a hardened stainless-steel vial (70 cm^3 in volume), filled with argon gas, and four stainless-steel balls (two with diameter of 1 cm and the other two with diameter of 0.7 cm). The ball to powder weight ratio is 7:1. The chemical composition of the final milled powder (milled for 30 h) was checked by energy dispersive analysis (EDS). The Fe concentration increases from 67 at.% of the starting sample to 69 at.% of the final product. Besides, 2 at.% of Cr impurities was observed.

XRD was measured for all the milled powders using Cu Kα radiation. The MS measurements were performed at RT and 4.2 K in the transmission geometry using a 57Co/Rh source. The velocity was calibrated by α-Fe. The spectra were fitted using the program written by Brand *et al* [9].

3. Experimental results

Figure 1 shows the XRD patterns of the as-filled and the milled Fe_2Hf powders. The as-filled powder can be indexed by the C14 $MgZn_2$ Laves structure. Upon milling, the diffraction lines broaden significantly indicating grain refinement. After 13 h milling, there is no obvious further change taking place in the diffraction patterns. For 30 h milled powder, XRD pattern show a crystalline structure phase which can be still indexed as C14 Laves phase.

The lattice parameters were obtained by the least-squares method from the most intensive lines of the XRD patterns. The results reveal that the lattice parameters decrease with milling time.

The RT Mössbauer spectra of the powders are shown in figure 3. For the as-filled powder, the Mössbauer spectrum displays two magnetic subspectra which are attributed, respectively, to Fe 6h and 2a sites in the Fe_2Hf intermetallic phase with C14 Laves structure [7]. The two subspectra exhibit hyperfine magnetic fields (B_{hf}) of 18.8 T (6h site) and 16.9 T (2a site). Upon milling, a non-magnetic component, labelled A, appears and it increases with milling time. This component shows a characteristic of quadrupole splitting distribution (QSD). For the powder milled for 30 h, the A component has a fraction of about 50% of the total absorption area.

It is also seen from figure 3 that, upon MM, the two subspectra of the starting phase become less resolved and, instead, a magnetic subspectrum D with B_{hf} distribution $P(B_{hf})$ presents. After 13 h milling, the subspectra from the initial phase are no longer observed and the spectra are composed of only the components A and D. The variation of the fractions of the residual starting phase as well as the components A and D as a function of milling time are displayed in figure 4. The fractions of these components are obtained from the fitting results. The error bars obtained from the fitting results are less than 2%.

Figure 5 shows the average isomer shifts $\langle IS \rangle$, related to α-Fe, of the starting intermetallic phase as well as the components A and D as a function of milling time. The $\langle IS \rangle$ of the starting phase has a value of about -0.186 mm s^{-1}. Upon milling, the $\langle IS \rangle$ of both components increases and, for the same powder, the $\langle IS \rangle$ of the component A is larger than that of D.

Figure 6 shows the 4.2 K Mössbauer spectra and the corresponding $P(B_{hf})$ curves of ball-milled powders. It is seen that the component A magnetically splits. The figure also shows that the position of the main peaks on the $P(B_{hf})$ curve does not change significantly with milling time, although the long-time-milled powders contain a large fraction of the component A. Figure 7 displays the average hyperfine magnetic field $\langle B_{hf} \rangle$ for the spectra displayed in figure 6. For comparison, figure 7 also includes the $\langle B_{hf} \rangle$ of the amorphous $Fe_{0.67}Hf_{0.33}$ alloy prepared by sputtering deposition [6]. One can see that the $\langle B_{hf} \rangle$ values of milled powders are smaller than the starting powder. It is also shown that, with the increase

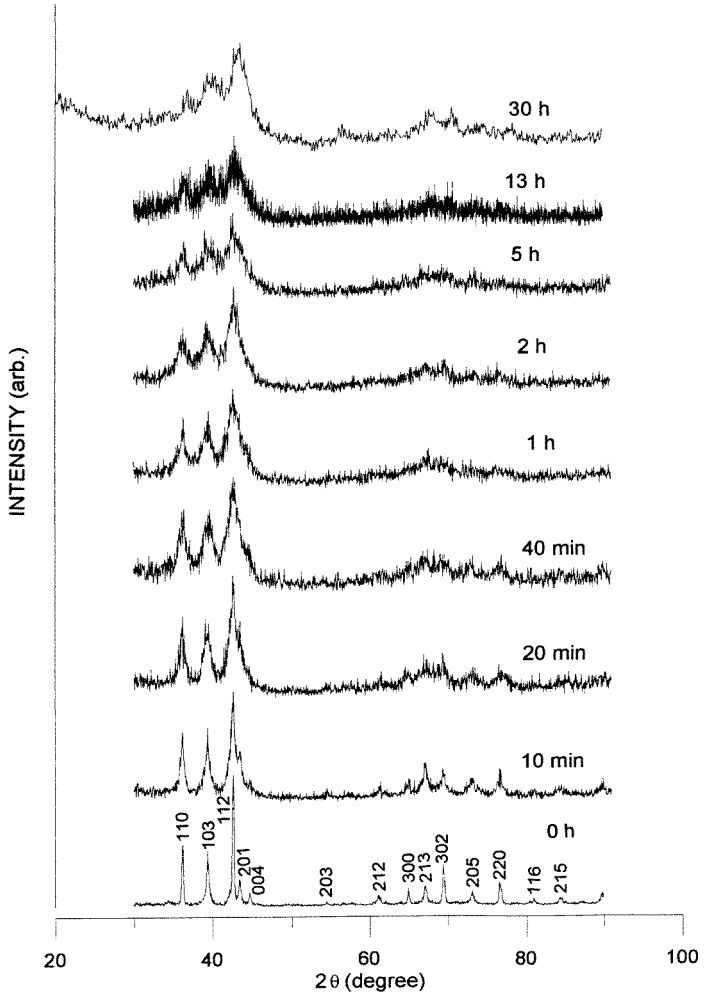

Figure 1. XRD patterns of the starting and the ball-milled Fe_2Hf intermetallic powders at the indicated milling times.

of milling time, the $\langle B_{hf} \rangle$ does not decrease monotonically. On the contrary, the $\langle B_{hf} \rangle$ of 30 h milled powder is even little larger than those of some short-time-milled powders. This reflects that the $\langle B_{hf} \rangle$ of component A is similar to or slightly larger than that of the component D.

The 4.2 K Mössbauer spectra were measured under applied magnetic fields with field direction parallel to the γ-ray for the 30 h milled powder, shown in figure 8, for determining the magnetic coupling behaviour. It is seen that the absorption lines 2 and 5 are undetectable when 0.5 T is applied and also the hyperfine field reduces with increase of applied fields. This is a ferromagnetic behaviour [10].

Figure 9 shows the RT Mössbauer spectrum measured under an applied magnetic field of 0.9 T with field direction perpendicular to the γ-ray direction, for the 30 h milled powder. The result indicates that the component A still maintains its non-ferromagnetic behaviour and its fraction of the absorption area. For the component D, the $\langle B_{hf} \rangle$ slightly reduces, as

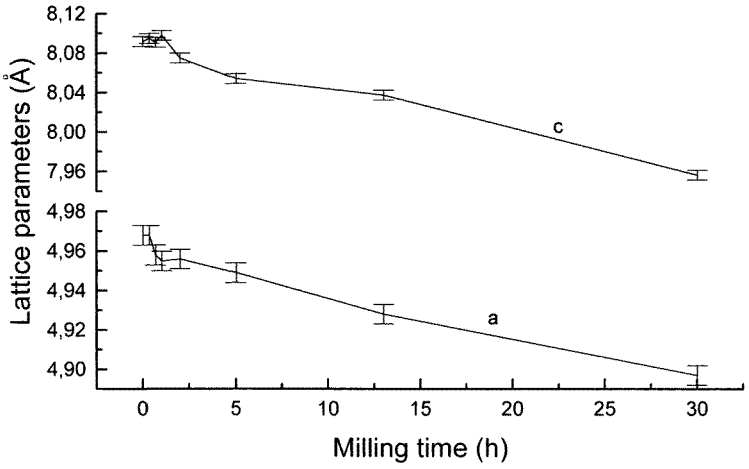

Figure 2. Lattice parameters of the crystalline phase of the ball-milled powders.

compared with that measured without applying field, because of the ferromagnetic behaviour mentioned above. The large ratio of the absorption line intensities between line 2 and 3 is due to the geometry of the experimental set-up between the applied field and the γ-ray directions.

4. Discussion

The above results indicate that MM leads to changes in atomic configurations of the starting intermetallic phase. The appearances of the component D (with B_{hf} distribution) and A (with QS distribution) result from distributions of atomic configurations, i.e. chemical disordering.

Chemical disordering can lead to changes in the IS of the milled powders (figure 5). The negative IS of an Fe–Hf alloy results from a transferring of s electrons from Hf sites to Fe sites, therefore, IS increases with the increase of Fe nearest-neighbour number as reported for the $Fe_{1-x}Hf_x$ amorphous alloys [8]. In the Fe_2Hf Laves phase, Fe atoms at both 6h and 2a sites are surrounded by 6 Hf atoms in their nearest neighbours, while the average number of Fe nearest neighbours around an Fe atom in a perfectly disordered alloy of the same structure or an amorphous phase is eight. Here both C14 Laves and amorphous phases have densely packed structure in which there are 12 nearest neighbours around each atom. Thus the increase of $\langle IS \rangle$ (figure 5) reflects the increase of the average Fe nearest-neighbour number, which is related to the degree of chemical disorder.

MM induced enhancement of lattice strain, attributed to the vacancies, dislocations etc, may also influence the IS. As suggested by Hellstern *et al* [11], the main contribution to lattice strain in ball milled intermetallics is the dislocation density. The maximum dislocation density in an alloy of about 10^{13} to 10^{14} cm^{-2} was observed in cold-rolled NiTi intermetallics by Koike *et al* [12], which corresponds to a nearest dislocation distance of about 2 nm. However, the dislocation density in a ball milled powder is considered to be much less than in a cold-rolled material [12, 13]. This is due to the fact that the temperature of the ball milled powders is higher than that of cold-rolled materials. Therefore, dislocation accumulation can occur during cold rolling; however, it does not take place in a ball milled powder since the dislocations, at the milling temperature, can became mobile

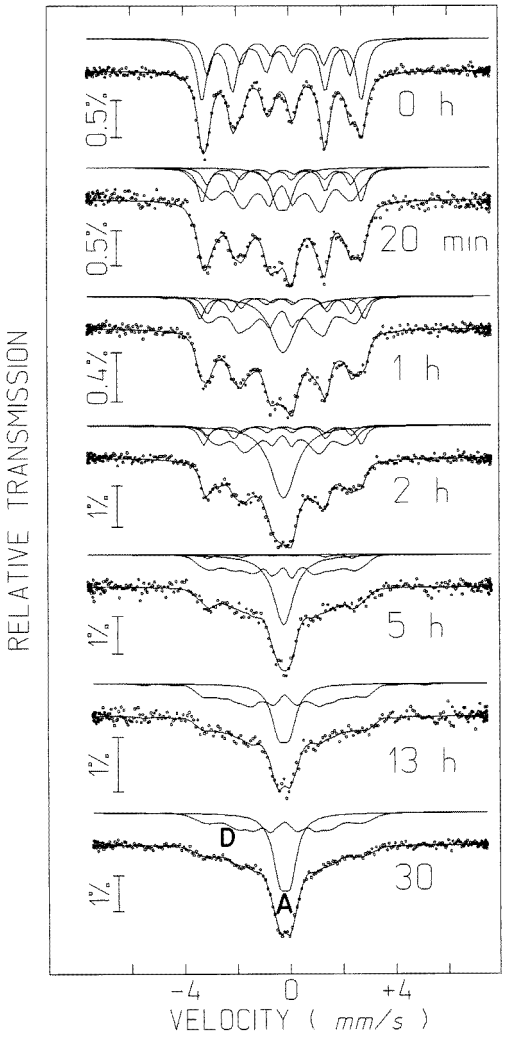

Figure 3. RT ^{57}Fe Mössbauer spectra of the ball-milled Fe_2Hf intermetallic phase.

and, as a consequence, disappear at grain boundaries. From this analysis one may expect that, although ball-milling induced a large amount of vacancies and dislocations, the fraction of atoms associated with these lattice defects is very small. Therefore, the effect of strain on the IS can be considered to be not significant.

The influence of the milling induced contamination by Cr and Fe on the IS should be also considered. It is known that introducing Cr into the Fe alloy also leads to a decrease in IS [14]. On the other hand, an increase of Fe concentration increases IS as mentioned above. Thus, considering the small amount of the contamination as well as the compromise of the two contributions to IS, one expects the contamination does not play a significant role to the measured IS.

For the same reasons mentioned above, the influences of the milling induced lattice defects and contamination on the B_{hf} can be also neglected. The modification of the B_{hf} upon milling is, therefore, related to the chemical disorder and structural variation.

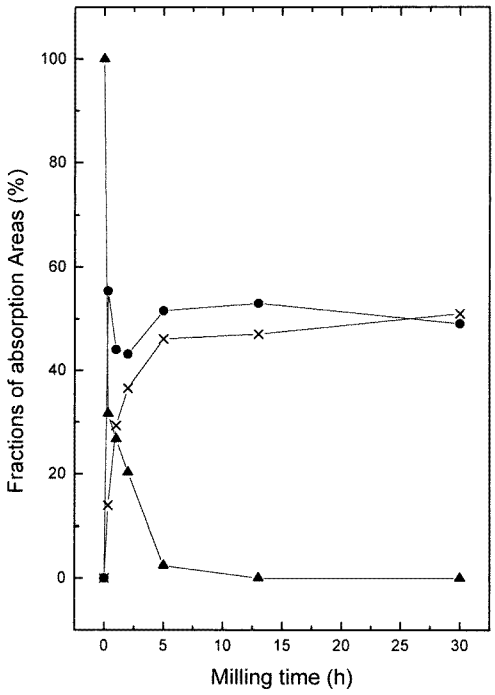

Figure 4. Mössbauer absorption fractions of the residual intermetallic phase (▲), the component A (×), and the component D (●).

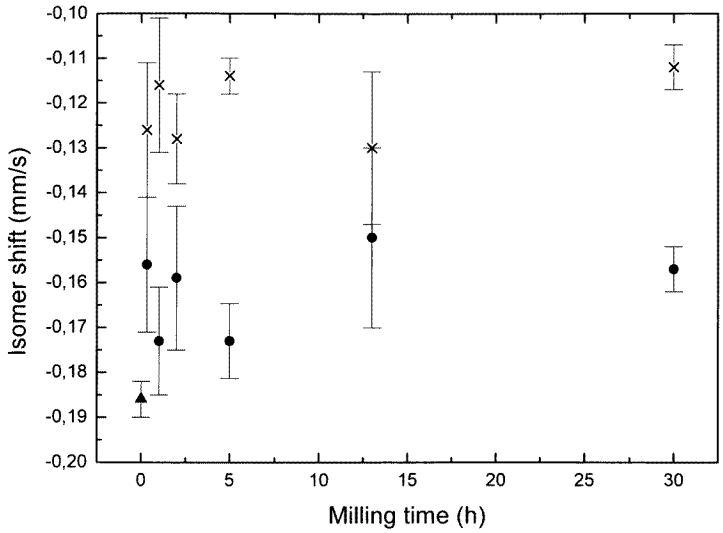

Figure 5. The average isomer shifts ⟨IS⟩ of the Fe_2Hf intermetallic phase (▲), the component A (×), and the component D (●).

Related to the structure of the ball milled powders, as the starting intermetallic phase, D is ferromagnetic above RT and the crystalline phase of the 30 h milled powder can be

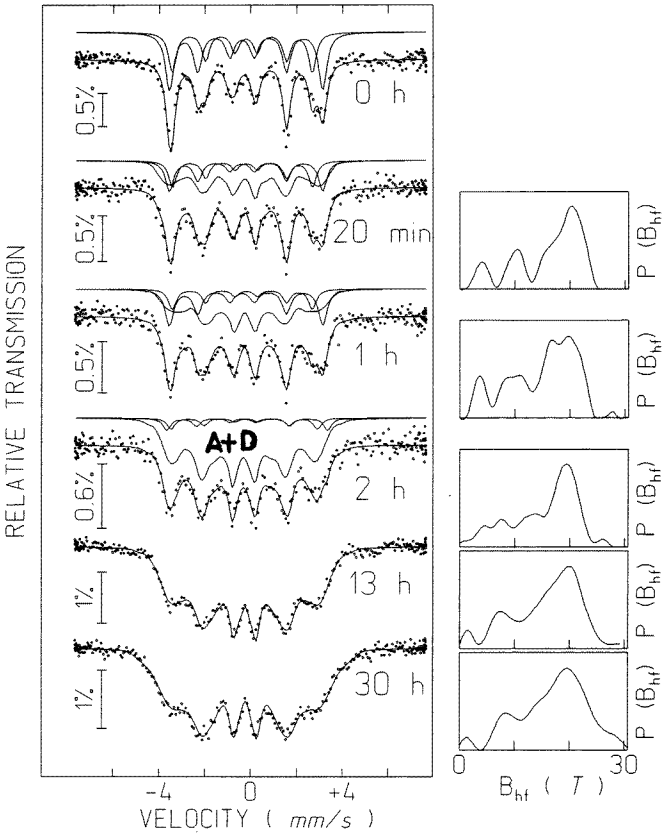

Figure 6. 4.2 K ^{57}Fe Mössbauer spectra of the ball-milled Fe_2Hf intermetallic phase and the corresponding $P(B_{hf})$ at the indicated milling times.

indexed as the C14 Laves lattice, therefore, the component D is attributed to a phase with C14 Laves structure. The slight increase in IS of the component D, as compared with the original intermetallic phase, indicates that a small degree of chemical disordering takes place. One can see that this phase has a slightly smaller $\langle B_{hf} \rangle$ compared with the starting compound.

The similar magnetic behaviour of A and D components (figures 6 and 7) at low temperature brings a question: whether the component A can be attributed to a superparamagnetic phase at RT. However, the RT Mössbauer measurement under an applied field (figure 9) excludes this possibility. Thus the atomic configuration of the component A will be different from the component D. Considering that 50% of Fe atoms is contained in the component A for the 30 h milling powder, while the XRD pattern, except the component D, does not show such a big quantity of any other crystalline phase (figure 1), one expects that the component A can be attributed to a structurally disordered phase, which is known as being non-ferromagnetic at RT [6]. In fact, closely checking the XRD pattern (figure 1), one finds that the diffraction pattern of the C14 Laves phase superposes on a broad halo pattern, which starts from about $2\theta = 30^\circ$ to 50°. Therefore, the halo pattern is attributed to the component A. However, compared with the $\langle B_{hf} \rangle$ (11.5 T) of the amorphous $Fe_{0.67}Hf_{0.33}$

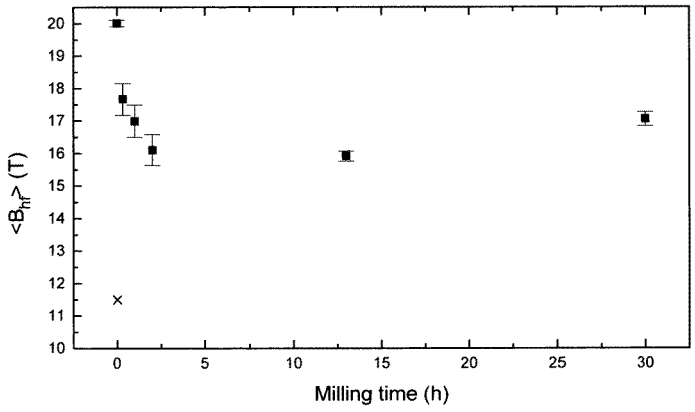

Figure 7. The average hyperfine magnetic fields $\langle B_{hf}\rangle$ over the total spectrum for each sample shown in figure 6. The $\langle B_{hf}\rangle$ of the amorphous $Fe_{0.67}Hf_{0.33}$ is also shown in the figure (×).

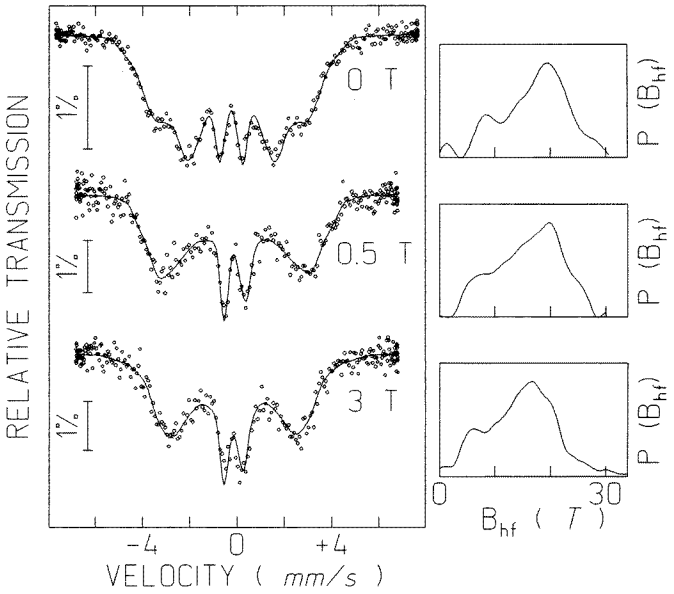

Figure 8. 4.2 K ^{57}Fe Mössbauer spectra measured under applied fields with field direction parallel to the γ-ray direction for the 30 h milled powders.

alloy prepared by sputtering deposition (figure 6), the $\langle B_{hf}\rangle$ value for component A is too large to be from an amorphous phase with the same composition. If the large $\langle B_{hf}\rangle$ value is attributed to a high-Fe-concentration amorphous alloy, the corresponding amorphous phase should have Fe concentration of more than 80 at.% [6], which has a IS of about -0.08 mm s^{-1} [8], a value much larger than that of the component A of -0.119 mm s^{-1}.

Since a sputtering deposited amorphous film can be approximately considered to be both structurally and chemically disordered, thus, the maintenance of the large $\langle B_{hf}\rangle$ of the component A may suggest that the component A has a disordered structure, but

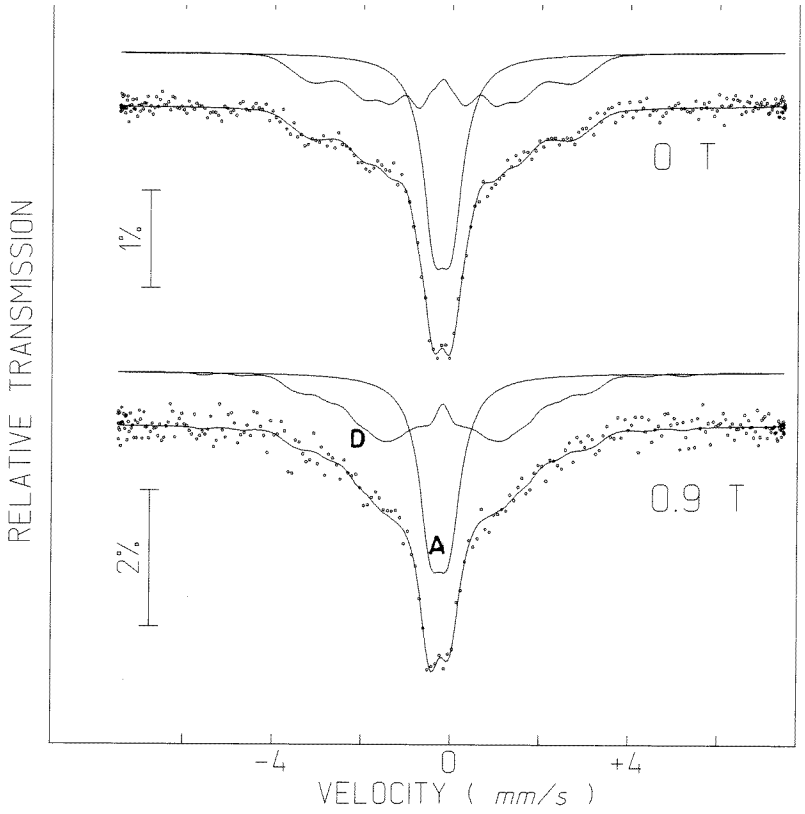

Figure 9. RT ^{57}Fe Mössbauer spectra measured under applied field of 0.9 T with field direction perpendicular to the γ-ray direction for the 30 h milled powders.

maintains considerable chemical short-range order. This explanation is also consistent with the prediction of Miedema's model [15, 16]. According to this model, the $Fe_{0.67}Hf_{0.33}$ alloy with a perfectly disordered crystalline structure has a higher free enthalpy than the same alloy with an amorphous structure. Thus, when chemical disordering reaches a certain degree at which the stored energy is comparable to the free enthalpy of the amorphous phase, structural disordering may occur and the chemical short-range order is maintained. A similar situation was also reported in several irradiated and ball milled intermetallic phases, such as CoZr [5], Zr_3Al [17] and $NiZr_2$ [18]. From this analysis, one expects that the component A is more chemically disordered than the component D.

The larger $\langle IS \rangle$ of the component A as compared with D is also an indication that the component A is more chemically disordered than D, as mentioned above. In the present case, the influence of the structural variation on the IS may be much less than that of the change in the atomic coordination because both C14 Laves and amorphous phases have densely packed structure. This can be seen by the similar $\langle IS \rangle$ values of the Fe_2Hf C14 Laves and the $Fe_{50}Hf_{50}$ amorphous phases [8]. Here, the $Fe_{50}Hf_{50}$ amorphous phase is compared with the Fe_2Hf C14 Laves phase because the average number of Fe nearest neighbours around each Fe atom in the former is the same as that in the latter. Further study on the atomic configuration by x-ray absorption spectroscopy (EXAFS) is being undertaken.

5. Conclusions

MM on the Fe_2Hf C14 Laves phase induces chemical disordering in the lattice and leads to a segregation of two phases. The phase with a lower degree of chemical disorder maintains the structure of the original intermetallic phase but has a little lower $\langle B_{hf} \rangle$. However, the phase with a higher degree of chemical disorder shows a disordered structure. This phase has a lower Curie temperature; however, it exhibits a $\langle B_{hf} \rangle$ much larger than that of the amorphous alloy with the same composition prepared by sputtering deposition. This is believed to be due to the existence of a considerable chemical short-range order in the structurally disordered phase.

Acknowledgments

The authors wish to acknowledge Professor M Forker for helpful discussion. This work was supported by grant No 301118/93-0-CNPq and grant No E-26/151.409/96-FAPERJ.

References

[1] Jang J S C and Koch C C 1990 *J. Mater. Res.* **5** 498
[2] Bakker H and Di L M 1992 *Mater. Sci. Forum* **88/89** 27
[3] Cho Y S and Koch C C 1993 *J. Alloys Compounds* **194** 287
[4] Xia S K, Baggio-Saitovitch E, Rodriguez V A, Passamani E, Takeuchi A Y, Ghfari M, Avillez R R and Assunção F C R 1996 *J. Alloys Compounds* **242** 85
[5] Zhou G F and Bakker H 1995 *Mater. Trans. JIM* **36** 329
[6] Liou S H, Xiao G, Talor J N and Chien C L 1985 *J. Appl. Phys.* **57** 3636
[7] Okamoto H 1993 *Phase Diagrams of Binary Iron Alloys* ed H Okamoto (Materials Park, OH: American Society of Metals) p 171
[8] van der Kraan A M and Buschow K H J 1983 *Phys. Rev.* B **27** 2693
[9] Brand R A J, Lauer J and Herlach D 1983 *J. Phys. F: Met. Phys.* **13** 675
[10] Ryan D H, Coey J M D and Ström-Olsen J O 1987 *J. Magn. Magn. Mater.* **67** 148
[11] Hellstern E, Fecht H J, Fu Z and Johnson W L 1989 *J. Appl. Phys.* **65** 305
[12] Koike J, Parkin D M and Nastasi M 1990 *J. Mater. Res.* **5** 1414
[13] Koch C C 1992 *Mater. Sci. Forum* **88–90** 243
[14] Bansal C, Campbell S J and Whittle G L 1988 *Hyperfine Interact.* **41** 551
[15] Loeff P I, Weeber A W and Miedema A R 1988 *J. Less-Common Met.* **140** 299
[16] Yang H and Bakker H 1992 *J. Alloys Compounds* **189** 113
[17] Schwarz R B and Johnson W L 1988 *J. Less-Common Met.* **140** 1
[18] Massobrio C 1990 *J. Physique. Coll.* **C4** 55